

**Contents**

|                                     |     |
|-------------------------------------|-----|
| 1. Introduction                     | 527 |
| 2. Material Description             | 528 |
| 3. Ground Strap Surge Current Tests | 528 |
| 4. Electron Swarm Tunnel Tests      | 540 |
| 5. Summary and Recommendations      | 546 |
| References                          | 547 |

## 8. Surge Current and Electron Swarm Tunnel Tests of Thermal Blanket and Ground Strap Materials

D.K. Hoffmaster, G.T. Inouye, and J.M. Sellen, Jr.  
TRW Defense and Space Systems Group  
Redondo Beach, Calif.

### 1. INTRODUCTION

This technical memorandum will describe the results of a series of current conduction tests with a thermal-control blanket to which grounding straps have been attached. The material and the ground strap attachment procedure will be described more fully in Section 2. The current conduction tests consisted of a surge current examination of the ground strap and a dilute flow, energetic electron deposition and transport through the bulk of the insulating film of this thermal blanket material. Both of these test procedures have been used previously with thermal control blanket materials. The surge current test procedure (and accompanying test results) has been previously described in Hoffmaster et al.<sup>1</sup> The electron deposition procedure (and accompanying results) has been described in Hoffmaster and Sellen.<sup>2</sup> Because of the length of these previous memoranda, there will be no attempt to represent here the content of these papers, and it is recommended that these earlier test procedures and results be read as a portion of the total TRW in-house examination of thermal control blanket material response to particle injection and to surge currents.

Without presenting specific experimental details here, it will be noted that the behavior of the material to these test procedures is considered as a distinct

improvement over previously observed behavior. Since the ultimate selection of spacecraft surface materials will, undoubtedly, involve many different features of the materials, superior performance to surge currents and deposited currents may **not** be the final, and crucial, material aspects. In view, however, of acknowledged problems in **charge** up discharge in magnetic substorms at geosynchronous altitudes, the material performance to **be described here** under certain simulations of these space environmental conditions should be considered as a strong reason for their use.

## 2. MATERIAL DESCRIPTION

The thermal control blanket material used here (ORCON KN-10) is a 0.0005 in. ( $1.27 \times 10^{-3}$  cm) Kapton\* film with a rear face of Vacuum Deposited Aluminum (VDA) to a depth of  $\sim 1000 \text{ \AA}$ . At the rear (exterior) face of the VDA film, a grid of NOMEX ribbon thread (described as a Mylar-like insulator) is attached. The grid is  $\sim 6$  threads per inch in each of two directions. The thread dimensions are  $\sim 0.0025$  in.  $\times$  0.020 in.

The ground straps are aluminum foil of 0.75 in. width and 0.002 in. thickness, bonded to the VDA layer with a conducting epoxy. The joints are overlaid with a 1.00 in.  $\times$  1.25 in. aluminum tape as per the current DSCS fabrication technique. Each kapton sample had an area of 3 in.  $\times$  4 in. and was equipped with two grounding straps.

## 3. GROUND STRAP SURGE CURRENT TESTS

### 3.1 General Considerations

In the surge current tests, the current is injected over a broad area at the midplane of the VDA film on the rear face of the Kapton and is conducted into a single ground strap. In principle, then, the current flow is in the VDA film and hence to the conducting epoxy and to the ground strap. In practice, it is apparent that, in addition to the conducting path above, current flow may also (if necessary) take place in the NOMEX grid.

The surge current generator is a power supply which charges a capacitor to 10,000 vdc and a hydrogen thyratron and series current limiting resistor. The firing of the hydrogen thyratron causes the capacitor to discharge through the

---

\*Some of the tests performed with the 0.0005 in. material were repeated with ORCON utilizing a 0.003 in. Kapton base film. See Section 4.3.2 for these tests.

series resistor ( $100\ \Omega$ ) and the VDA film/conducting epoxy/aluminum ground strap. The total charge flow is determined by the capacitance and the charging voltage. For the capacitors used of  $3.6 \times 10^{-9}$ ,  $10.0 \times 10^{-9}$  and  $100 \times 10^{-9}$  F and the charging voltage of 10,000 volts, it follows that total charge flows for the various tests were  $\sim 36$ , **100**, and  $1000\ \mu\text{C}$ . The characteristic durations of these current surges were  $\sim 0.36$ , **1.0**, and  $10.0\ \mu\text{sec}$ .

Two types of resistance measurements were made. The first of these is a steady-state measurement from the input clamp to the output clamp on the surge current generator, made after each current-burst. Only very low sensing voltages are used in these measurements. The second resistance measurement is a "dynamic" measurement, and is made during the time of the high current passage through the VDA/ground strap combination. Significant differences may exist between these two measurements, particularly at the high burst number level, where the removal of VDA near the ground strap bond has taken place.

### 3.2 Steady State Resistance

Ohmmeter type measurements were carried out on six ground straps. The results of these resistance measurements are given in Figures 1 through 6 as a function of the number of current bursts applied and for the three levels of capacitance in the high voltage storage capacitor.

Figures 1 and 2 illustrate results for a  $3600\ \text{pF}$  capacitor, charged to 10,000 volts and with a series resistance of  $100\ \Omega$  (leading to a peak surge current of **100 A**). The shape of the  $R(n)$  curve is similar to those obtained previously. For a large number of bursts, the steady state, post-burst, resistance remains approximately constant. Above some burst number, however, increases in resistance are comparatively rapid. In previous tests of ground straps, these rapid increases in resistance were attributed to the removal of the last remaining portions of the VDA film leading into the conducting epoxy bond.

While removal of VDA occurs for the present samples (as well as for previous ones), there are two major differences between the behavior observed here for the added NOMEX grid and the previous samples where the grid has been absent. The first major difference is that the number of bursts required to reach the "knee" of the  $R(n)$  curve is now considerably larger than for the previous ground straps. For example, (see Figure 7, Hoffmaster et al<sup>1</sup>), the knee of  $R(n)$  curve for  $3.6 \times 10^{-9}$  F,  $100\ \Omega$ , and  $10^4$  volts was observed at  $\sim 300$  bursts for the ground straps used there, while in the present case, over 1000 bursts were required to reach the rapid rising portions of  $R$  versus  $n$ .

A second major difference between present and previous results is that, for the present (NOMEX added) ground strap, visible surface arcs did not occur, even

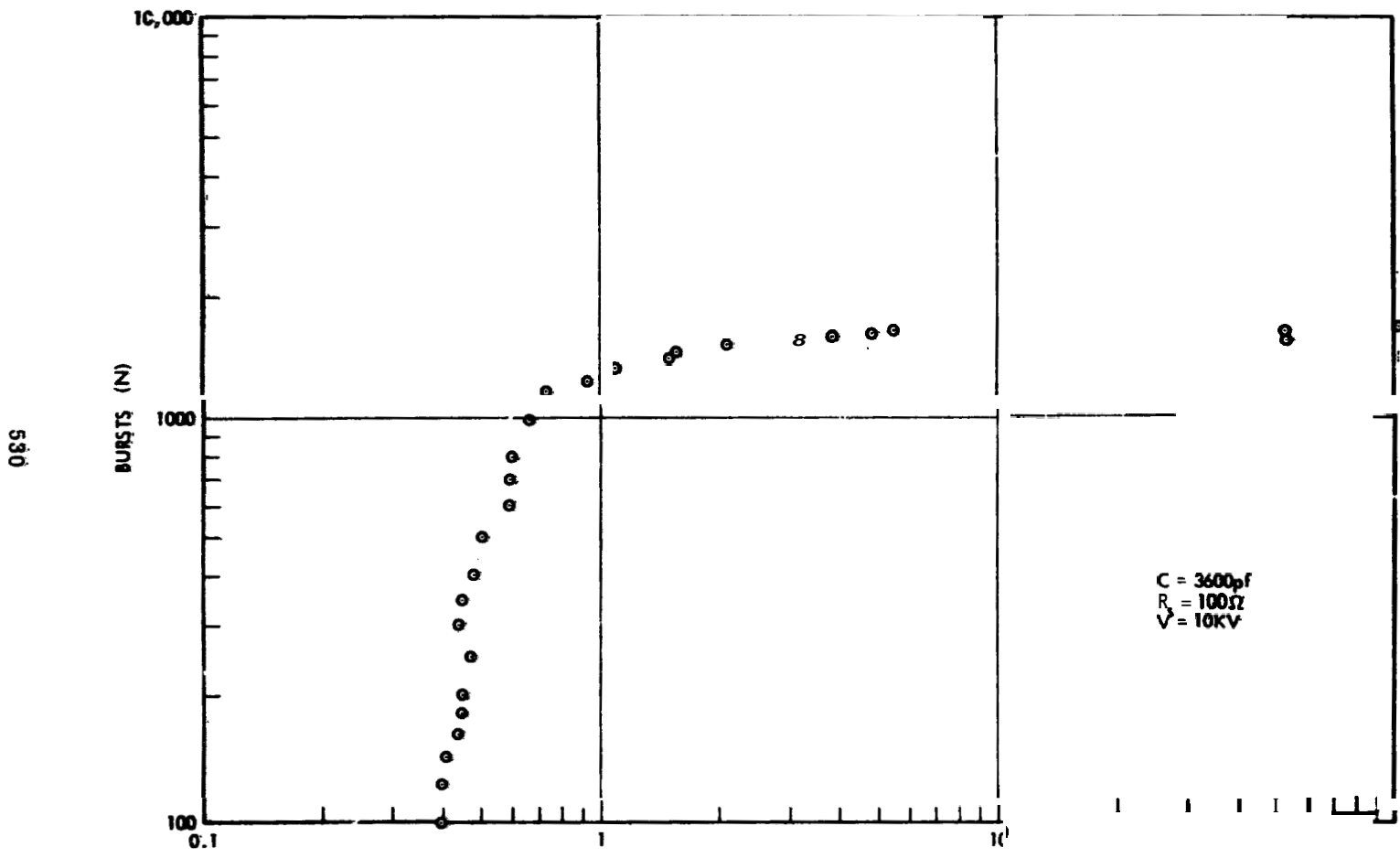


Figure 1. Resistance of VDA/NOMEX/Groundstrap Sample 1 as a Function of the Number of Current Burets. Initial surge current = 100 A and total charge throughput = 36  $\mu$ c

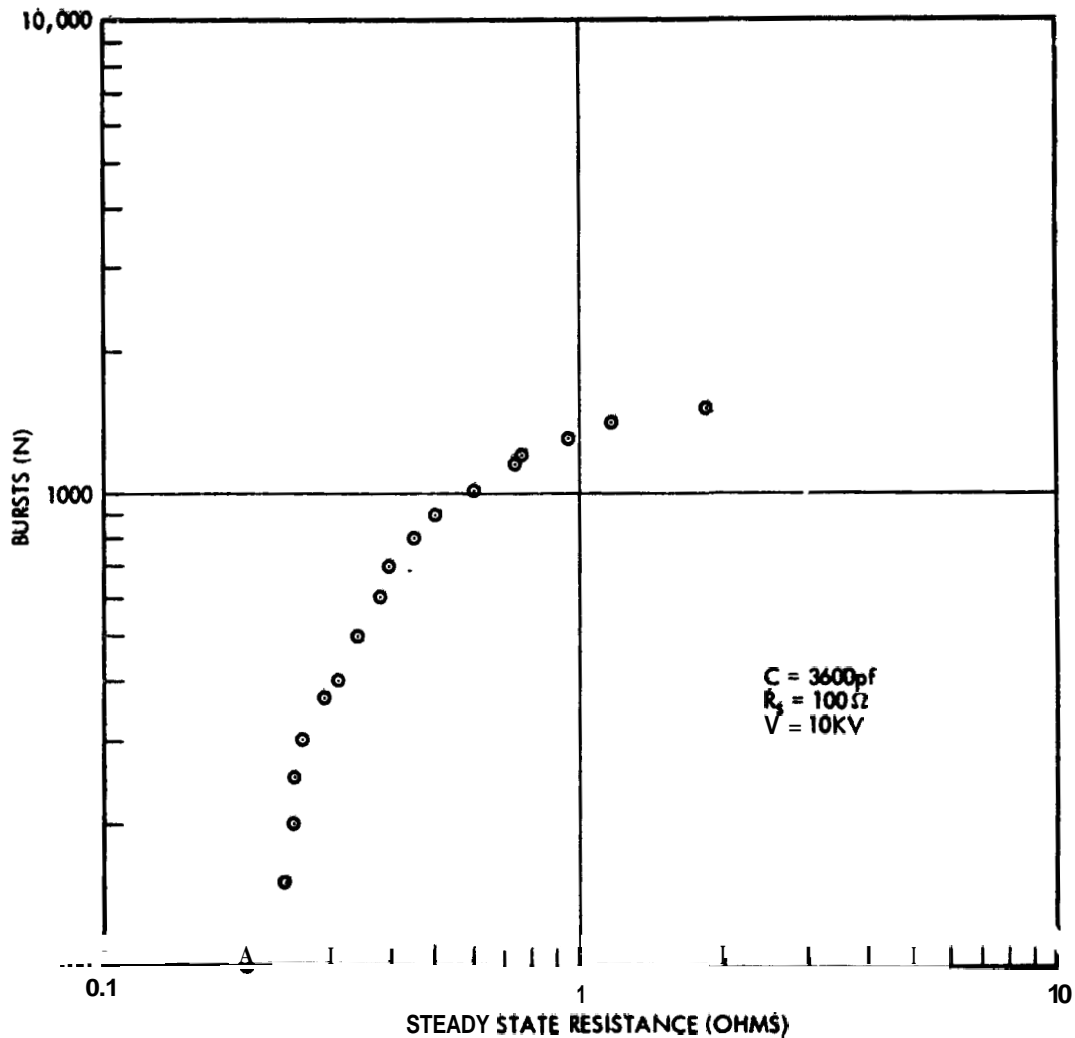


Figure 2. Resistance of VDA/NOMEX/Groundstrap Sample 2 as a Function of the Number of Current Bursts. Initial surge current = 100 A and total charge throughput = 36  $\mu$ c.

after the VDA film had been removed from the region of the bond. It is apparent that the presence of the NOMEX grid provides alternative conduction paths and that the conduction of this dew conduction does not result in the metal-to-metal arcs across dielectric surfaces observed earlier. This is a significant improvement in performance and indicates a large reduction in surface discharge current noise, should conduction be required and if the VDA film near the bond has been removed by previous current bursts. Section 3.3 will consider these dynamic current conduction processes further.

Figures 3 and 4 illustrate the steady state resistance as a function of the number of bursts for a larger capacitor than above. The increase in C from  $3.6 \times 10^{-11}$  to  $10 \times 10^{-9}$  F results in a loss of ground strap life. VDA film removal now occurs at  $\sim 300$  bursts. When the capacitance is increased to  $100 \times 10^{-9}$  F, the film removal occurs after  $\sim 20$  bursts. These results are given in Figure 5. Visible surface arcs were not observed for these higher capacitance discharges, following

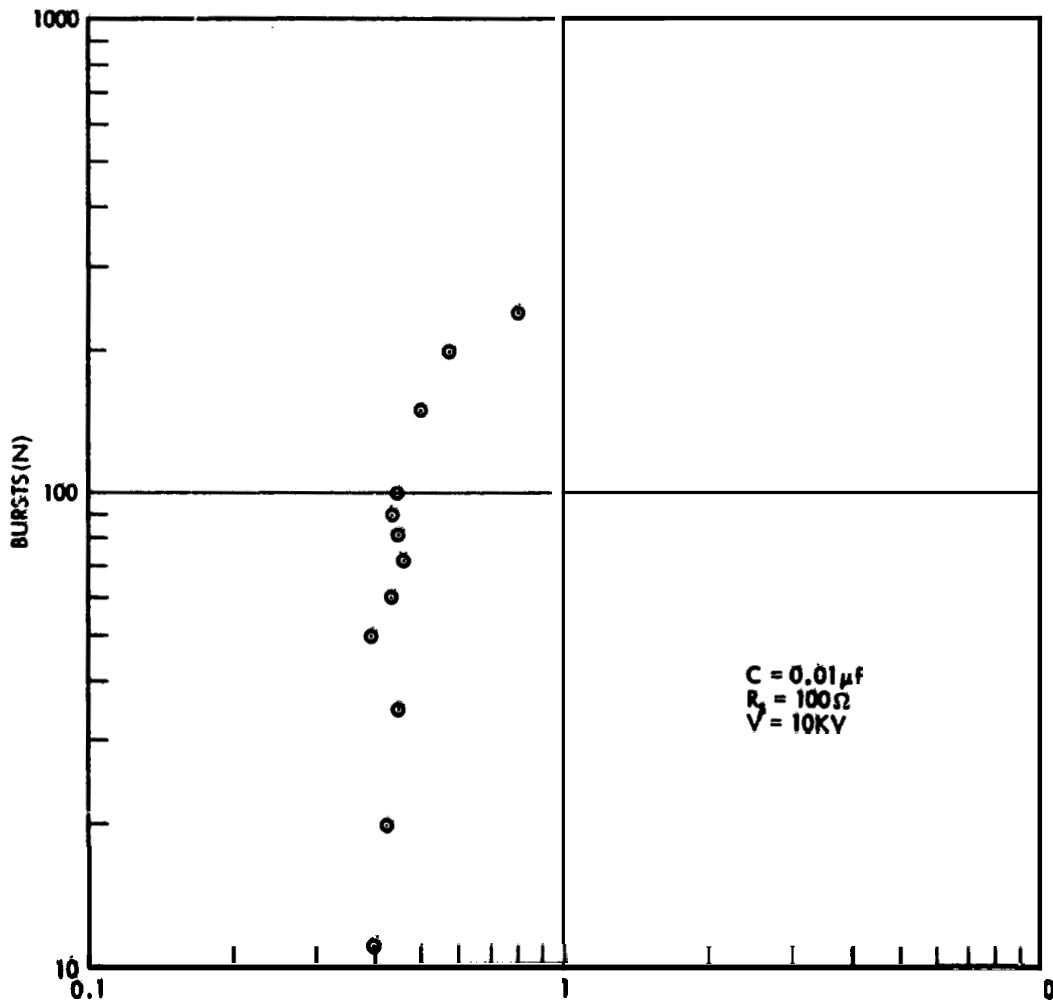


Figure 9. Resistance of VDA/NOMEX/Groundstrap Sample 3 as a Function of the Number of Current Bursts. Initial surge current = 100 A and total charge throughput = 100 μc

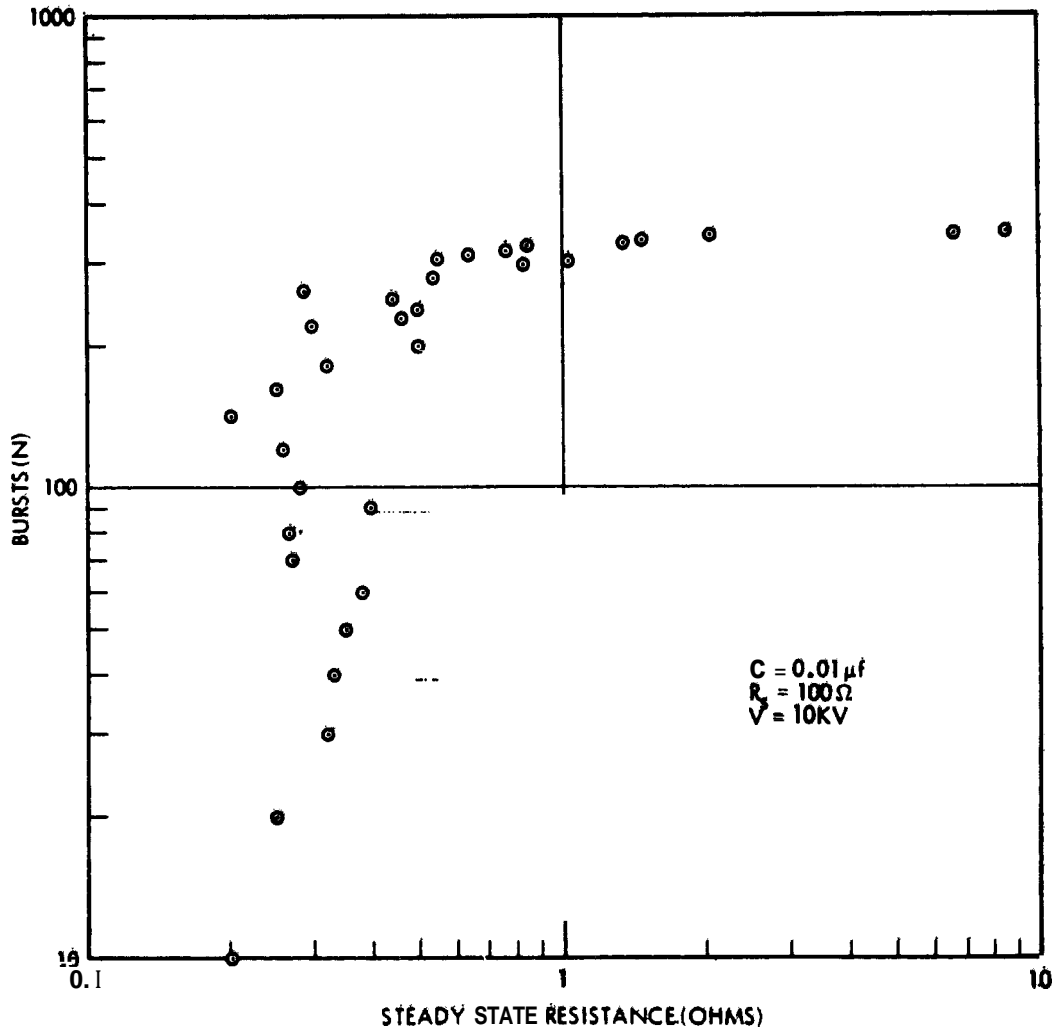


Figure 4. Resistance of VDA /NOMEX/Groundstrap Sample 4 as a Function of the Number of Current Bursts. Initial surge current = 100 A and total charge throughput = 100  $\mu c$

loss of VDA and the increase in the steady state resistance. The loss of allowable burst number before VDA removal with increasing capacitance is expected to occur and had been observed previously in the ground strap experiments of Hoffmaster et al (see, for example, Figure 9, of Hoffmaster<sup>1</sup>). The most significant feature, however, for this newer configuration is a conduction ability after VDA removal and without surface breakdown.

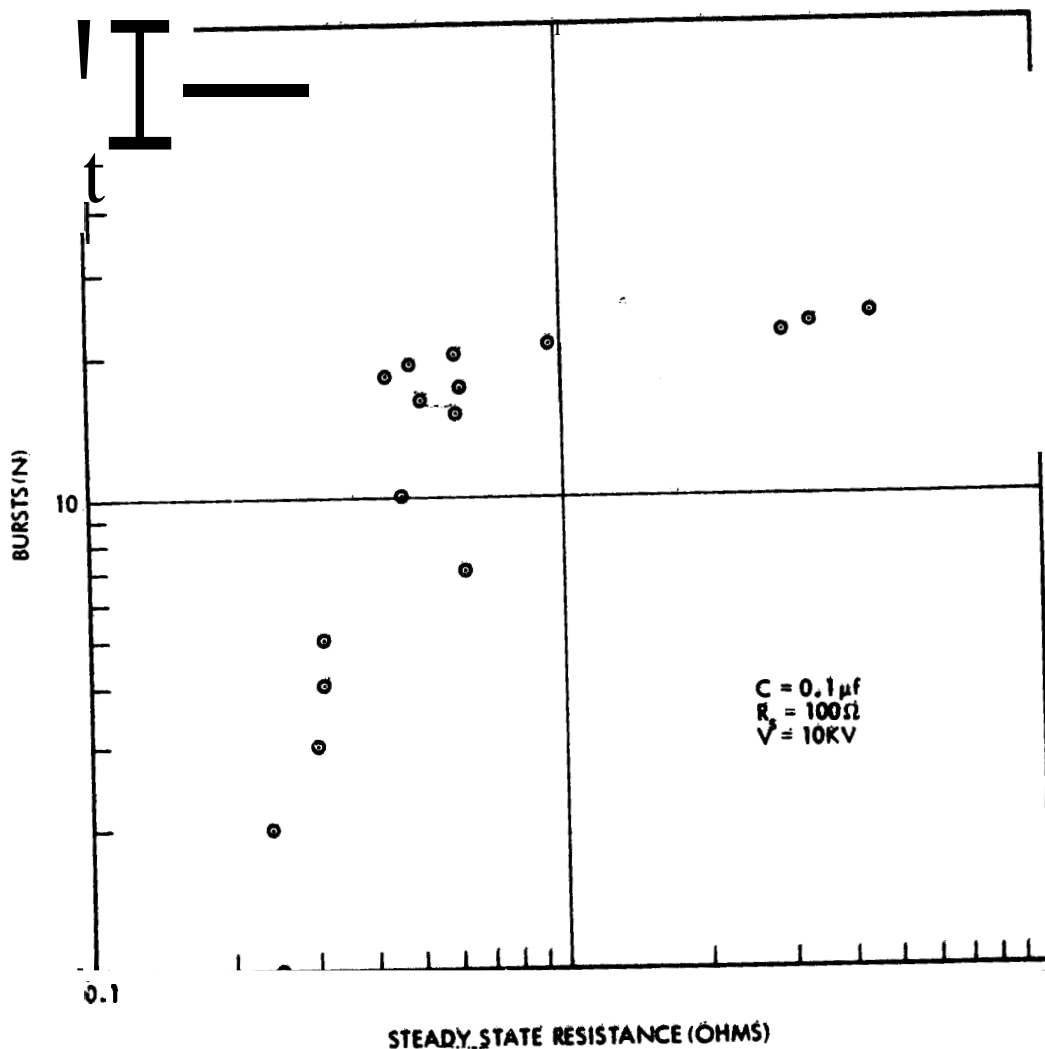


Figure 5. Resistance of VDA/NOMEX/Groundstrap Sample 5 as a Function of the Number of current Bursts. Initial surge current = 100 A and total charge throughput = 1000  $\mu c$

### 3.3 Dynamic Resistance

The dynamic resistance measurements are obtained by measured current flow in the circuit and the accompanying clamp-to-clamp voltage during the current burst. This dynamic resistance will not be equal to the steady state resistance, in general, and, also of importance, will not remain at the same value during the current burst. To illustrate the differences between steady state and dynamic

resistances, this section will contain measurements of both, although principal emphasis will be on resistance during the current burst.

For these measurements, a fresh sample, (Sample No. 6), was examined for both steady state and dynamic values as a function of burst number and as a function of time during the current burst. Figures 6 - 9 have the results of these measurements. In Figure 6, the conventional, steady state, resistance is given. For a capacitance of 10,000 pF,  $10^4$  volts, and 100  $\Omega$  in series resistance, this sample withstood in excess of 400 bursts before exhibiting a deterioration of the VDA film. Excess of 900 bursts were required to reach high level steady state resistance.

The dynamic resistance was measured at three time periods, 0.33  $\mu$ sec, 0.94  $\mu$ sec, and 2.5  $\mu$ sec after the initiation of the current burst (Figures 7 - 9). Two effects are apparent. The first of these is a diminution of dynamic resistance for later periods in the burst conduction, and is evidence in a change in the surface material properties. The second effect is that dynamic resistance proceeds to values significantly less than the post burst steady state resistance.

The exact nature of the surface change taking place during the burst has not been determined. There is no visible surface arc. There is, nevertheless, some surface (or perhaps NOMEX) alteration which provides an increasingly effective conduction path for current, for increased flow duration, and which acts, after the VDA removal, as an effective, alternate, conduction path.

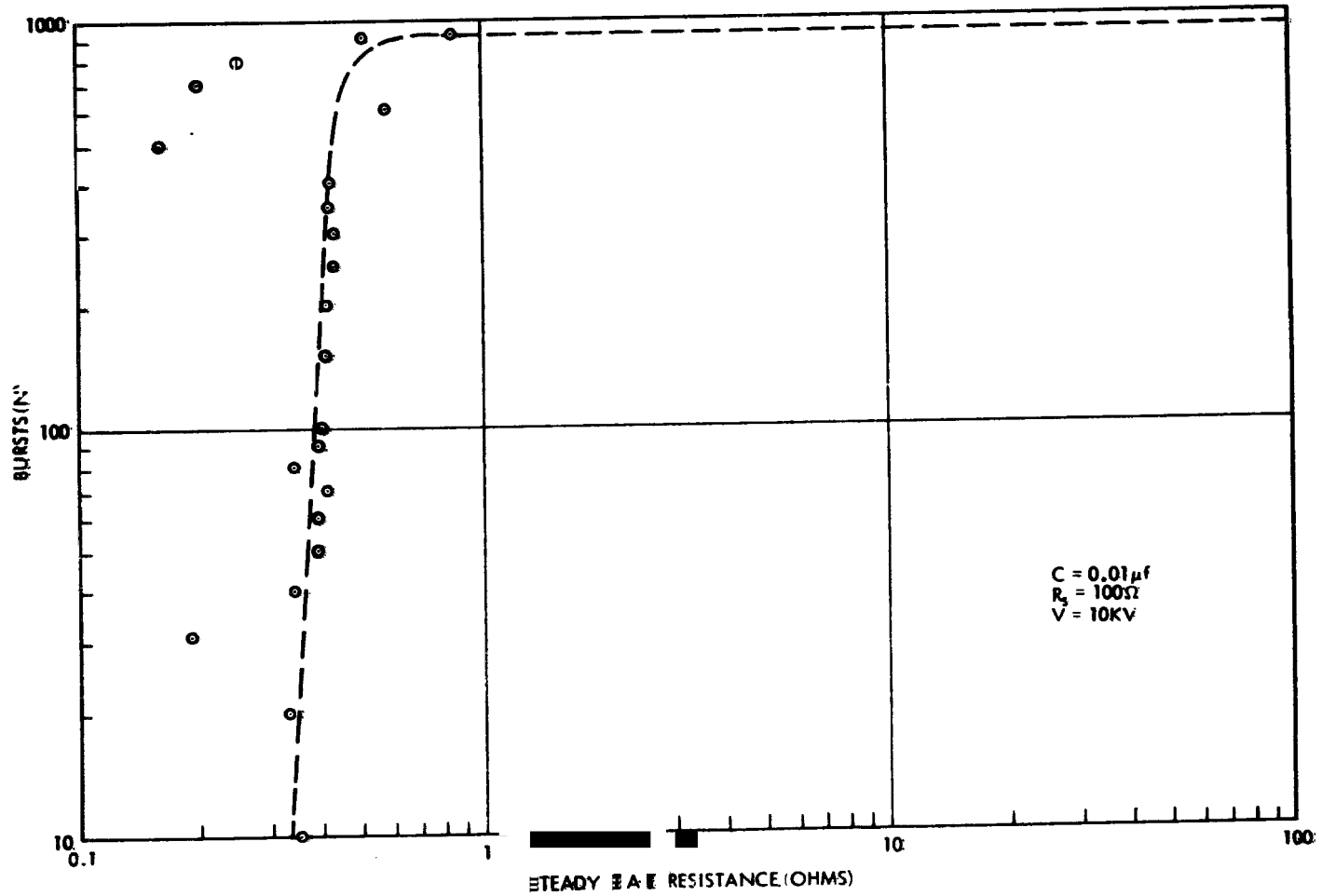
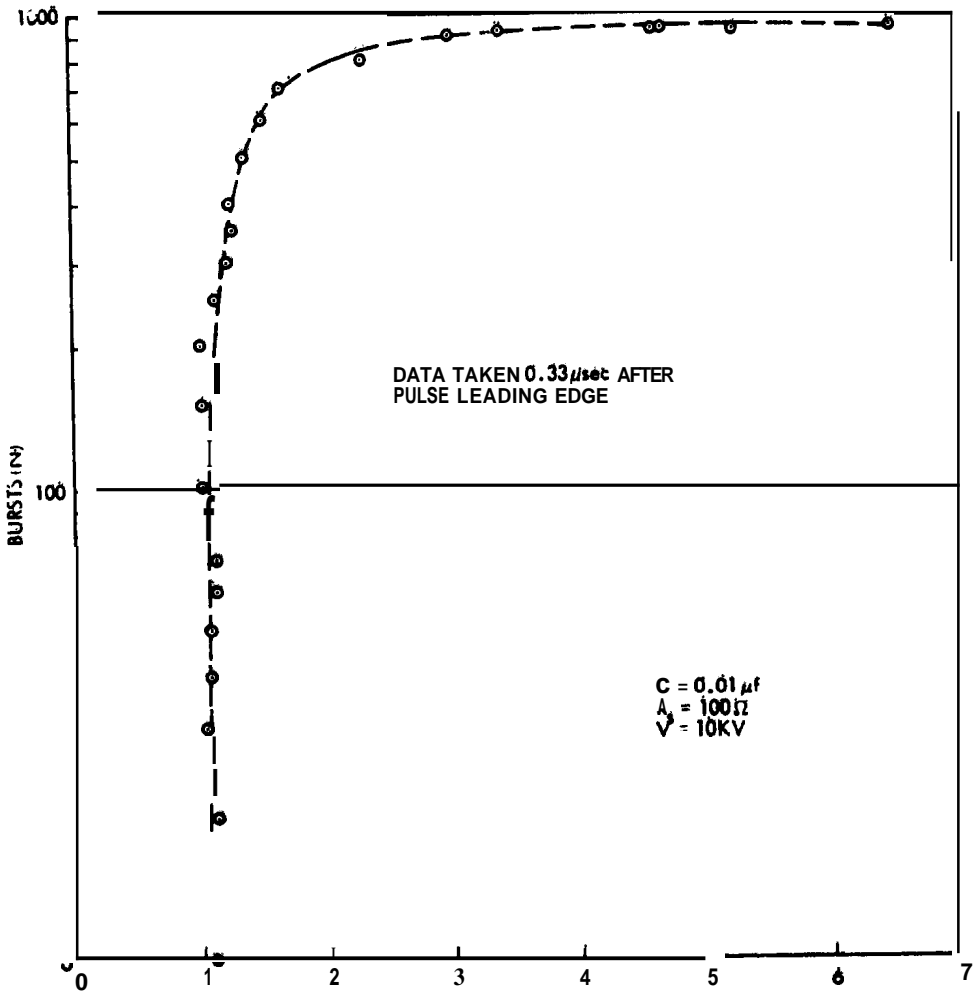
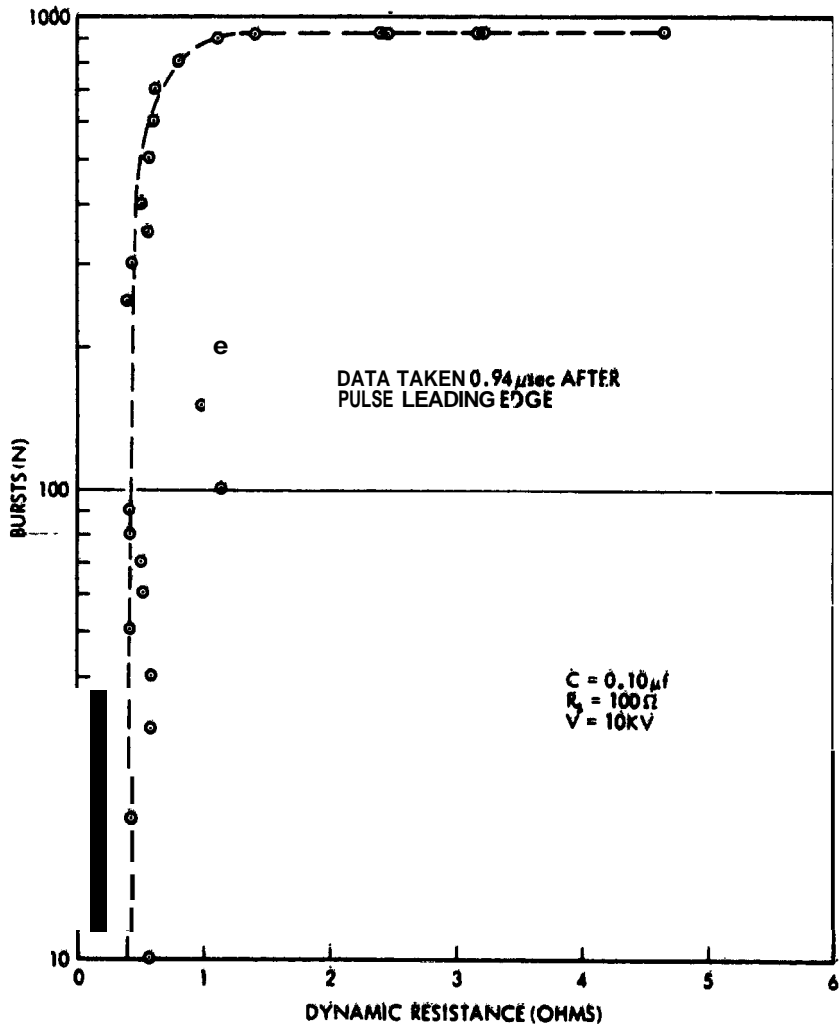


Figure 6. Resistance of VDA/NOMEX/Groundstrap Sample 6 as a Function of the Number of Current Bursts. Initial surge current = 100 A and total charge throughput = 100  $\mu c$





**Figure 8. Dynamic Resistance of VDA/NOMEX/Groundstrap Sample 6 as a Function of the Number of Current Bursts at 0.94  $\mu$ sec after Current Surge Initiation**

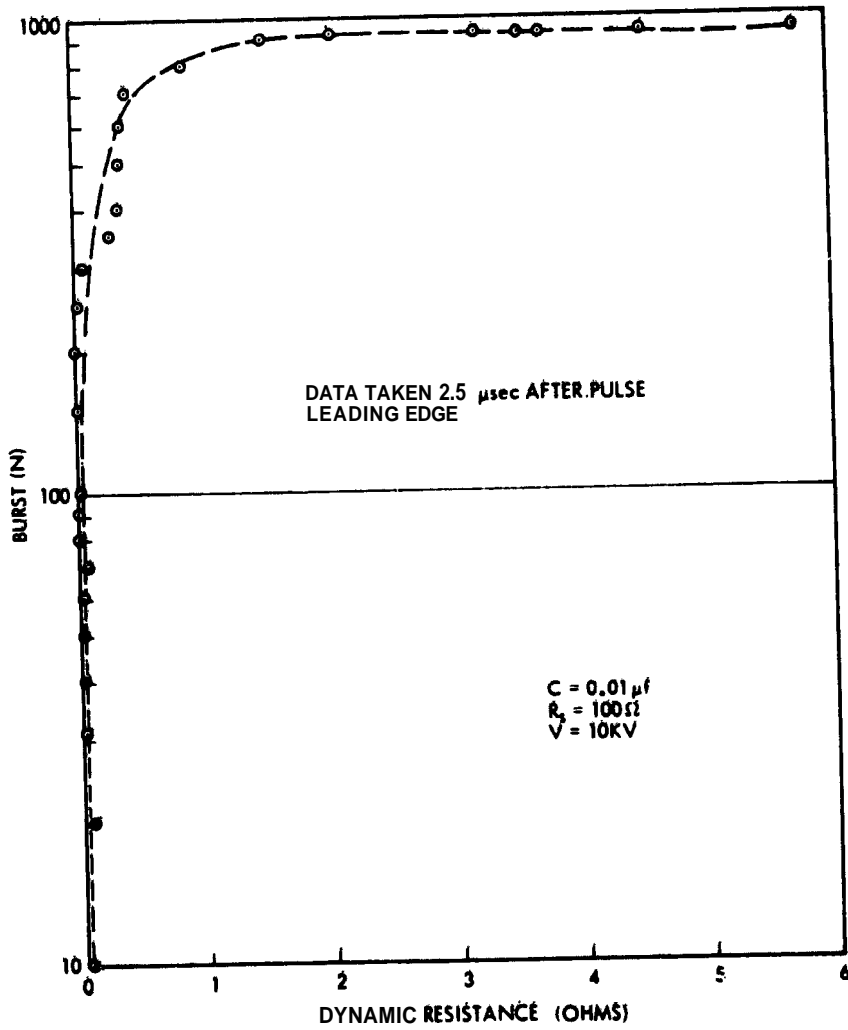


Figure 9. Dynamic Resistance of VDA/NOMEX/Groundstrap Sample 6 as a Function of the Number of Current Bursts at 2.5  $\mu\text{sec}$  after Current Surge Initiation

## 4. ELECTRON SWARM TUNNEL TESTS

### 4.1 General Considerations

The results of the current surge tests indicated that the presence of the NOMEX grid on the rear face aids in conduction of these large current bursts. In the process of grid attachment, however, it appeared as a possibility that the NOMEX grid could cause a field intensification for electrical conduction through the bulk of the Kapton film which could (possibly) result in dielectric-to-metal arcs from the Kapton interior to the rear face VDA for severe charge-up on the Kapton surface. The Electron Swarm Tunnel (EST) tests were initiated to explore this second, and important, charge conduction process.

The EST used for these tests is the 2 ft X 4 ft facility described earlier in Hoffmaster and Sellen.<sup>1</sup> In this chamber, a monoenergetic electron beam streams along the chamber axis and deposits on the exterior face of the dielectric film, thus simulating the electron deposition process during magnetic substorms in space. In the 2 ft X 4 ft EST, both electron flux and electron energy are variable. Although light sources are present in this facility, there was no deliberate application of light during the electron deposition, and, thus, no deliberate appeal to photoconductive transport of deposited electrons through the foil. In the deposition tests to be discussed here, electron acceleration energy varied from 2 to 6 keV and deposition flux from  $10 \text{ nA/cm}^2$  to  $20 \text{ nA/cm}^2$ .

### 4.2 Sample Configuration

Figure 16 illustrates the sample configuration used in the EST tests. The measured drainage current is at the rear face VDA film for forward face electron deposition. The added ring on the front surface (with overlying insulating films) acts as a guard ring to prevent surface drainage current entrance into the rear face VDA film. The resulting measurements are, thus, of bulk conduction currents in the Kapton as a result of the deposition of energetic electrons on the front surface of the film.

### 4.3 Electron Drainage Current Measurements

#### 4.3.1 DRAINAGE THROUGH KAPTON AT 0.0005 IN. THICKNESS

Figure 11 illustrates the drainage current density (in nanoamperes per square centimeter) as a function of the acceleration voltage of the deposited electrons and for varying levels of electron flux in the deposition. The order in which the exposures have been made is significant.

The initial deposition condition was a 2 keV electron flow at  $10 \text{ nA/cm}^2$ , leading to a rear face drainage current of  $\sim 0.05 \text{ nA/cm}^2$ . This drainage current is

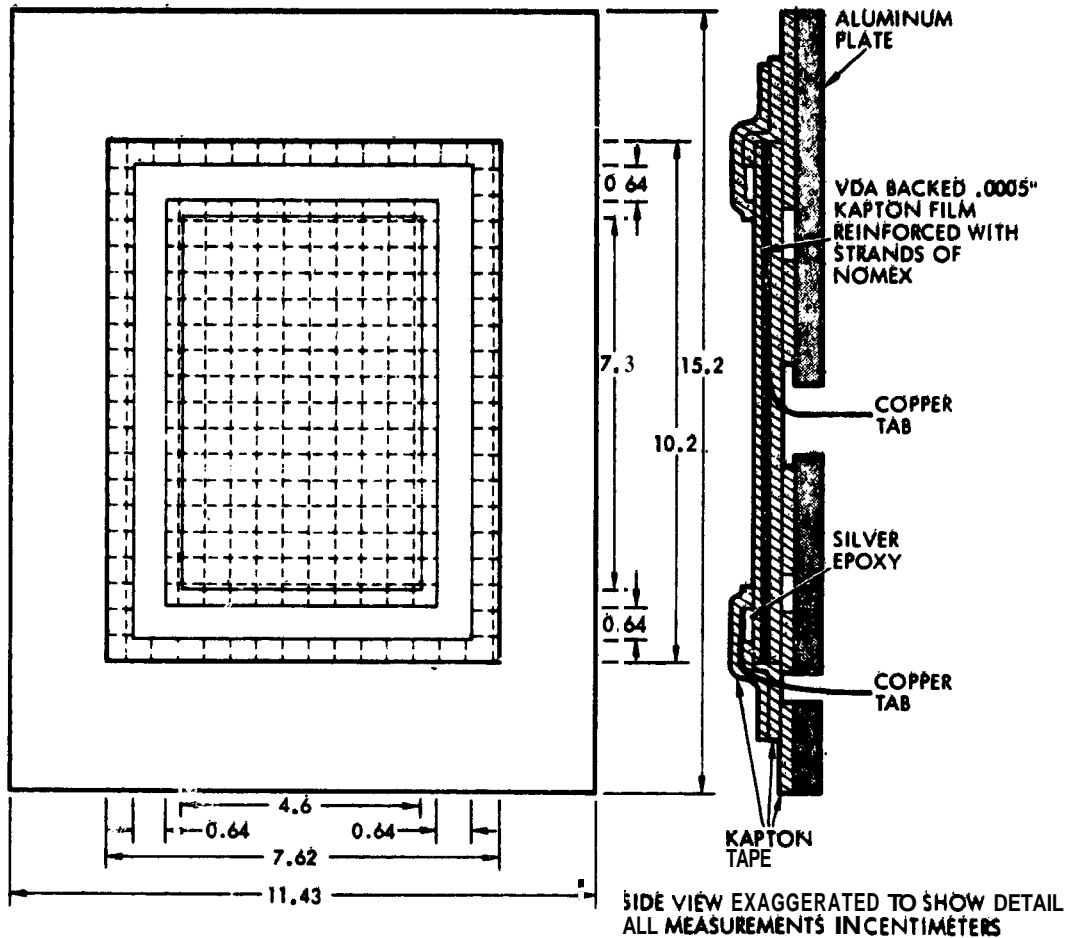


Figure 10. Kapton/VDA/NOMEX Thermal Control Material Sample Configuration for Electron Swarm Tunnel Tests

considerably larger than that observed for 0.002 in. ( $5 \times 10^{-3}$  cm) Kapton foil, measured earlier. Larger drainage is expected, of course, because of the reduced thickness ( $1.27 \times 10^{-3}$  cm) of the foil.

Increases in beam energy to 4 keV caused drainage current density to increase to  $\sim 0.5 \text{ nA/cm}^2$ . This rapid increase in conduction current density as beam energy increased is typical, and is attributed to field enhanced conductivity in the material. A continued increase in electron acceleration energy to 6 keV, caused an increase in conduction current to  $1.5 \text{ nA/cm}^2$ . Since the incident flux at this point was only  $10 \text{ nA/cm}^2$ , and since secondary electron emission causes a rerelease, back to space, of significant amounts of electrons, the observed

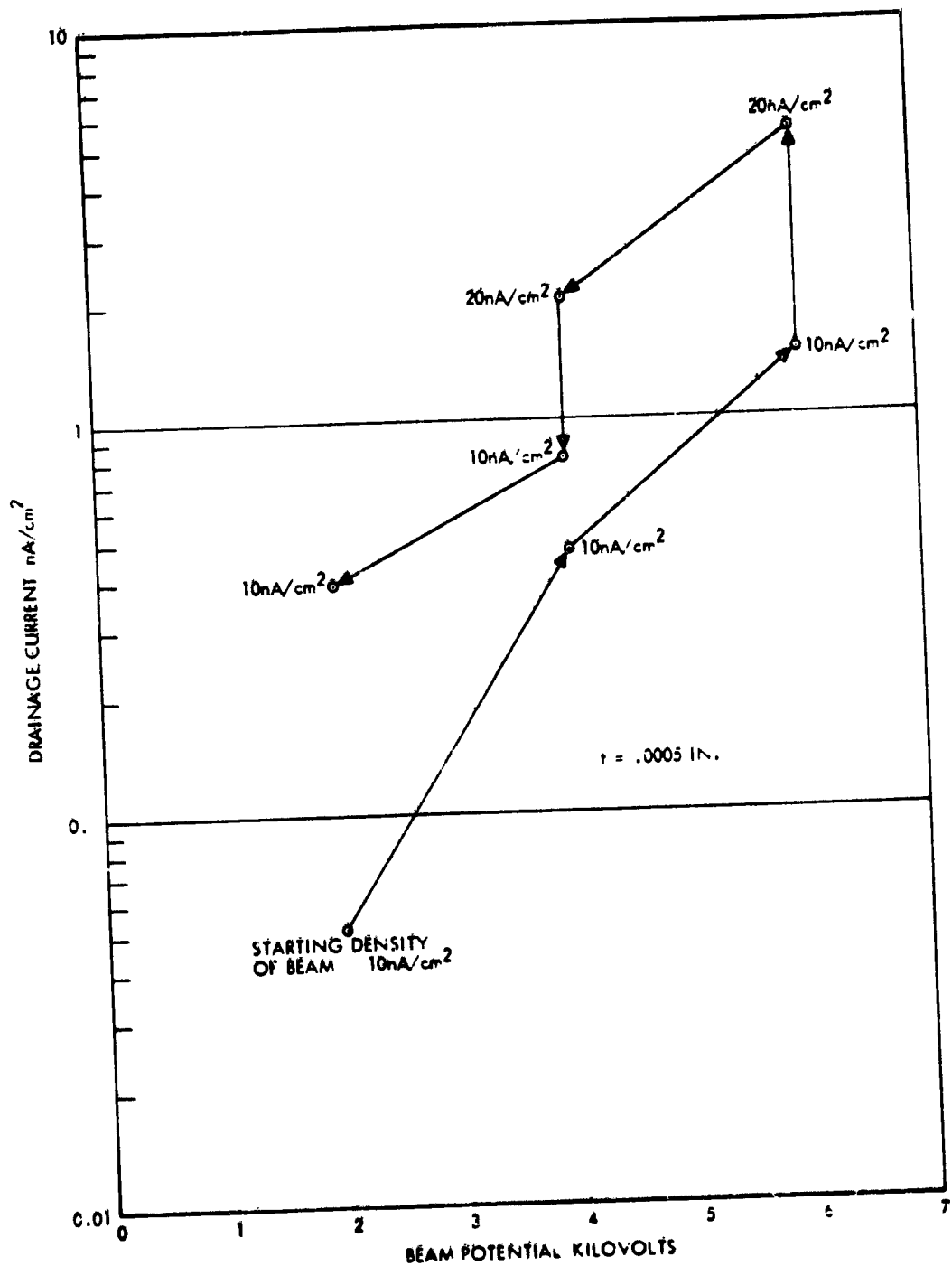


Figure 11. Electron Drainage Current Density as a Function of Electron Beam Acceleration Voltage for Deposition Flux Densities of 10 nA/cm<sup>2</sup> and 20 nA/cm<sup>2</sup> on ORCON Utilizing 0.0005 in. Kapton Base Film

conduction could be limited by incident flux rather than by material resistivity. To test this possibility, the deposition flux was increased from  $10 \text{ nA/cm}^2$  to  $20 \text{ nA/cm}^2$  and conduction current density increased from 1.5 to  $5.4 \text{ nA/cm}^2$  thus (confirming notions of conduction limited to incident deposition).

These extraordinary drainage levels (in excess of substorm depositions) usually lead to material alteration. To examine the possibility of permanent alteration, the deposition conditions were then moved to (4 keV,  $20 \text{ nA/cm}^2$ ) to (4 keV,  $10 \text{ nA/cm}^2$ ) and, finally, to (2 keV,  $10 \text{ nA/cm}^2$ ). The evidence clearly demonstrates that a permanent alteration of the material has occurred as a result of the high level drainage at the upper end point of the acceleration voltages applied.

The drainage current measurements also examined the conduction current trace for evidence of material electrical breakdown. Although occasional alterations of drainage current were observed, there were no major interruptions. At the conclusion of the drainage current tests, the sample was removed from the test chamber and subjected to visual and microscopic examination. There was no evidence of electrical breakdown. This is not to conclude that optical properties (absorptivity, emissivity) of the Kapton film have remained unaltered by the high electric stress electron drainage conduction. Measurement of optical properties should be carried out both before and after the electron deposition to determine if film alteration has occurred.

#### 4.3.2 DRAINAGE THROUGH KAPTON AT 0.003 IN. THICKNESS

Section 1 has noted that the ultimate selection of spacecraft surface materials will involve many different features of the materials. Mechanical strength of the base film is amongst those features. At the conclusion of the tests with the 0.0005 in. Kapton film sample described in the sections above, and concurrent with the availability for test of a material similar to the first sample (NOMEX grid and VDA features unchanged) but with 0.003 in. thick Kapton as the base film, it was considered of interest to repeat the current conduction tests. The surge current conduction behavior would not appear likely to be dependent upon the base film thickness, because these surge currents are within the VDA film and the NOMEX fibers. There was no apparent reason, thus, for a repetition of the surge current conduction for the ORCON film utilizing the thicker Kapton as the base film. The bulk conduction of electrons through the film in the EST tests, on the other hand, could be expected to be thickness dependent, and these electron deposition experiments were repeated with the new, thicker film, samples.

The 0.003 in. Kapton film ORCON sample construction was the same as that illustrated in Figure 10, except that the Kapton film, as previously noted, is not 0.003 in. thick, and the lateral dimensions of the sample whose drainage is under examination are  $7.1 \times 7.1 \text{ cm}$  (rather than the  $4.6 \times 7.3$  dimensions used in the 0.0005 in. base film case).

The second ORCON sample was placed in the EST and the beam energy varied from 4 to 10 keV at current densities of 10 nA/cm<sup>2</sup> and 20 nA/cm<sup>2</sup>. Figure 12 illustrates the measured conduction current in this sample with the thicker Kapton film. Several features of the results shown there differ considerably from the drainage current results shown in Figure 11 for the thinner Kapton. The major difference between the two films is that the drainage current density is greatly reduced for the thicker film, compared to the drainage of the 0.0005 in. sample. Under a conventional approach to this electron conduction it might be expected that drainage currents would be reduced by a factor of 6, because the film thickness increases by a factor of 6 (0.0005 in. to 0.003 in.) and because film resistance in conventional conduction should be proportional to film thickness. It should be noted, however, that the conduction is reduced by ratios much larger than the thickness ratio. At 4 keV, 10 nA/cm<sup>2</sup> conditions the drainage current densities are ~0.5 nA/cm<sup>2</sup> for the thin material and 0.009 nA/cm<sup>2</sup> for the thicker material. At 6 keV, 10 nA/cm<sup>2</sup> conditions, the respective drainage current densities are 1.5 nA/cm<sup>2</sup> and 0.025 nA/cm<sup>2</sup>. The ratio of the drainage current densities at 4 keV is 55 and at 6 keV is 60, which in both instances is very much larger than the thickness ratio of 6.

The marked drop in electron drainage as material thickness  $t$  increases, appears to be the result of field dependent bulk resistivity. It has been previously noted in these drainage experiments that bulk resistivity is clearly nonconstant for electric stress values above some critical upper bound. The field point at which conduction increases rapidly is considered to be near  $10^5$  V/cm. For the thinner film this condition is attained for ~125 Volts from one face of the film to the other. For the thicker film,  $\Delta V \sim 10^3$  volts, before the  $10^5$  V/cm point is attained. For  $E > 10^5$  V/cm, the bulk resistivity appears to decline as  $\exp\{-K\sqrt{E}\}$ , possibly as the result of Poole-Frenkel effect. Irrespective of the exact cause of the extra conduction, however, it should be emphasized that the thinner film has a much larger electric stress as a result of e-beam deposition than for the thicker film, and, hence, will conduct substantially larger drainage currents.

A second major difference between the behavior of the two sample thicknesses is in the permanent material alteration observed for the thinner film as a result of the e-beam exposure, while the thicker Kapton sample returns to the same drainage level when the e-beam deposition conditions are returned to earlier voltage and flux levels (the order of exposure for the thicker film was 4 keV, 10 nA/cm<sup>2</sup>; 6 keV, 10 nA/cm<sup>2</sup>; 8 keV, 10 nA/cm<sup>2</sup>; 16 keV, 10 nA/cm<sup>2</sup>; 10 keV/20 nA/cm<sup>2</sup>; 8 keV, 26 nA/cm<sup>2</sup>; 6 keV, 20 nA/cm<sup>2</sup>; and 6 keV, 10 nA/cm<sup>2</sup>). The "closure" experiment at 6 keV, 10 nA/cm<sup>2</sup> revealed no permanent material change for the thicker sample, while the thinner sample exhibited almost one order of magnitude

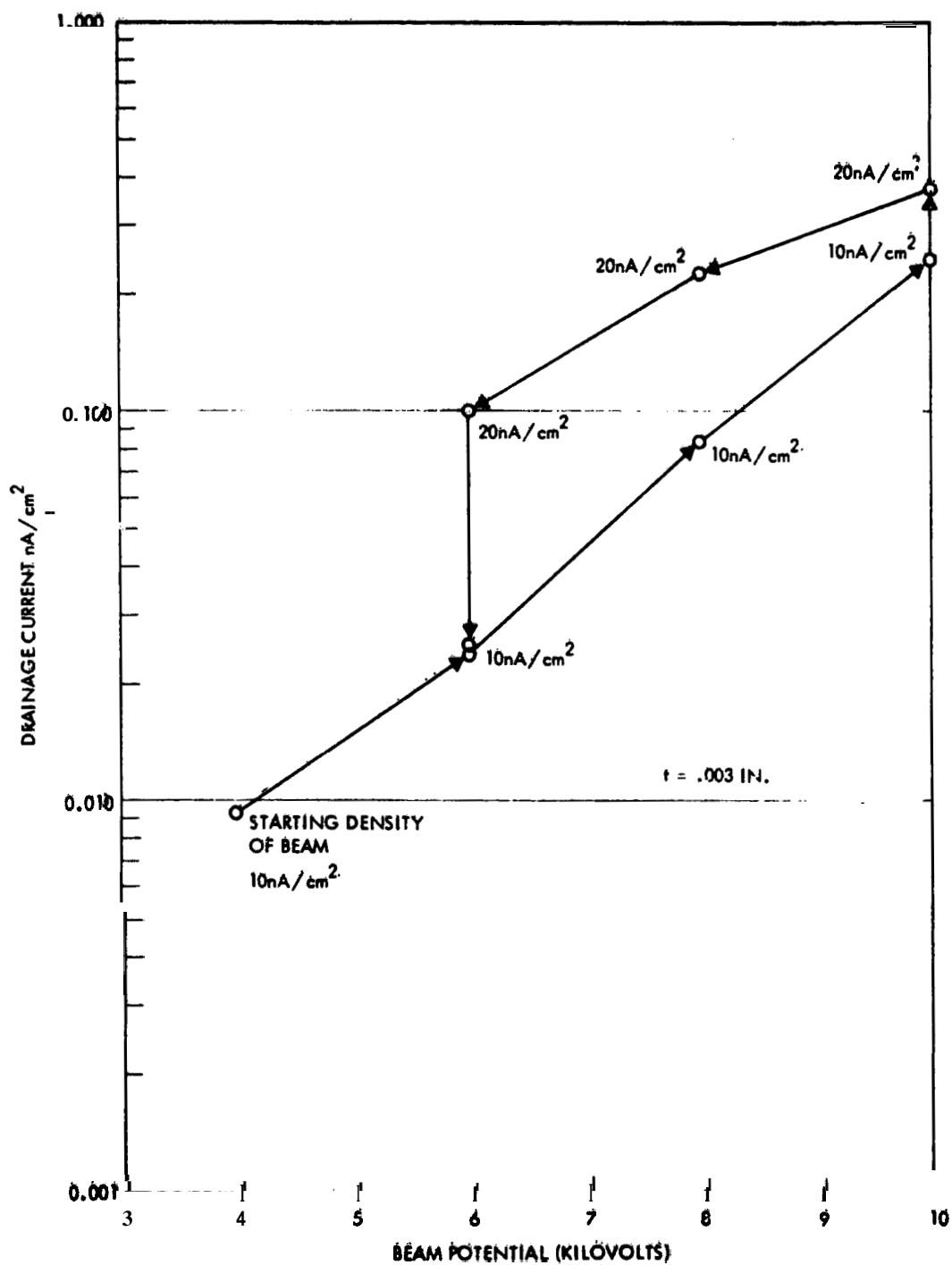


Figure 12. Electron Drainage Current Density as a Function of Electron Beam Acceleration Voltage for Deposition Flux Densities of 10 nA/cm<sup>2</sup> and 20 nA/cm<sup>2</sup> on ORCON Utilizing 0.603 in. Kapton Base Film

change from its two 2 keV,  $10 \text{ nA/cm}^2$  exposures, and a factor of approximately 2 at the 4 keV,  $10 \text{ nA/cm}^2$  conditions (see Figure 11).

From the results given in Figures 11 and 12 it is apparent that the thinner material has much higher drainage currents than the thicker material, and that permanent alteration has taken place in the thinner material. These results are encouraging from the standpoint of the use of the 0.003 in. Kapton. A remaining question is the possible occurrence of dielectric-to-metal arcs in the thicker material. To monitor the possible occurrence of such breakdowns in the film, the drainage currents were continuously displayed on Chart recorders. There was no evidence of material breakdown in the recorded drainage current traces. Following the e-beam tests, the sample was removed from the test chamber and visually examined for pinhole breakthroughs. There was no visible evidence that any such breakthroughs had occurred. Measurements of  $\alpha$  and  $\epsilon$  were not carried out and should be included in future e-beam deposition tests. From the present evidence it would appear that permanent alteration in the material did not occur, either in observed drainage currents or in visible punch-throughs.

## 5. SUMMARY AND RECOMMENDATIONS

The response of the rear face VDA film/NOMEX/ground strap configuration to surge currents has been examined and found to be superior to that of earlier VDA/ground straps. More bursts are allowed before ground strap resistance begins its sharp rise, and, even after the removal of the VDA, conduction occurs (presumably through the NOMEX) without surface breakdowns.

The forward face Kapton layer of the 0.005 in. ORCON material was exposed to an EST beam ranging from 2 to 6 keV with fluxes of  $10 \text{ nA/cm}^2$  and  $20 \text{ nA/cm}^2$ . Drainage currents were large and increased with continued exposure to the electron deposition, indicating a material change. There was no evidence, however, of dielectric to metal arcs. There were no measurements of surface absorptivity or emissivity, so there is no way of determining at present if these quantities altered as a result of the electron deposition. These measurements should be carried out. The forward face Kapton layer of a 0.003 in. ORCON material was also exposed to an EST beam. For this material the beam energy ranged from 4 to 16 keV. The observed drainage currents were greatly reduced compared to the thinner Kapton film. There was no evidence of permanent film alteration in the bulk conduction as a result of the e-beam deposition, and examination of the drainage current traces and visual examination of the sample failed to reveal any evidence of dielectric to metal arcs.

The behavior of this material was generally superior to that of previous film/  
bonding/ground strap configurations in the surge current tests. In the electron  
drainage measurements of bulk conduction, the 0.003 in. Kapton sample was  
considerably superior in performance to that of the 0.0005 in. thickness sample.  
From the results of these measurements the use of the NOMEX grid backing is  
indicated as desirable and the thickness of Kapton should be the 0.003 in. case  
rather than the 0.0005 in. material.

## References

1. Hoffmaster, D.K., Komatsu, G.K., Roy, N.L., and Sellen, J.M., Jr. (1974) Surge Current Conduction in Vacuum Deposited Aluminum Films Bonded Aluminum Ground Straps, TRW 4351.3.74-34.
2. Hoffmaster, D.K., and Sellen, J.M., Jr. (1974) Electron Swarm Tunnel Measurements of Kapton Bulk Resistivity at High Electric Stress Levels, TRW 4351.3.74-59.